

7N-31  
104034  
P-19

**NASA  
Technical  
Paper  
3249**

June 1992

# Definition and Design of an Experiment To Test Raster Scanning With Rotating Unbalanced-Mass Devices on Gimbaled Payloads

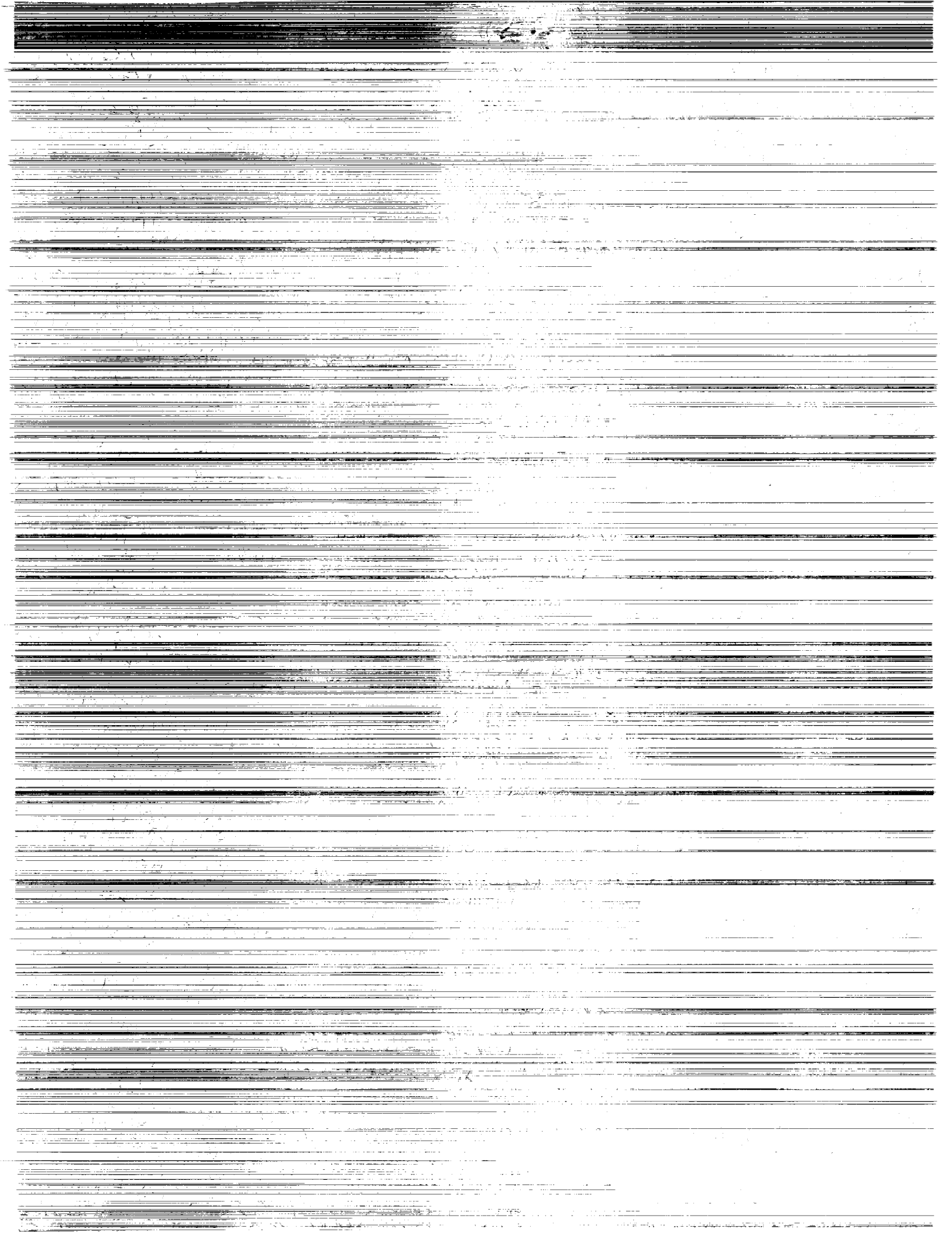
W. D. Lightsey,  
D. C. Alhorn,  
and M. E. Polites

(NASA-TP-3249) DEFINITION AND DESIGN OF AN EXPERIMENT TO TEST RASTER SCANNING WITH ROTATING UNBALANCED-MASS DEVICES ON GIMBALED PAYLOADS (NASA) 19 p

N92-29677

H1/31 Unclas  
0104034





**NASA  
Technical  
Paper  
3249**

1992

**Definition and Design of an  
Experiment To Test Raster  
Scanning With Rotating  
Unbalanced-Mass Devices  
on Gimbaled Payloads**

W. D. Lightsey,  
D. C. Alhorn,  
and M. E. Polites  
*George C. Marshall Space Flight Center  
Marshall Space Flight Center, Alabama*



National Aeronautics and  
Space Administration  
Office of Management  
Scientific and Technical  
Information Program

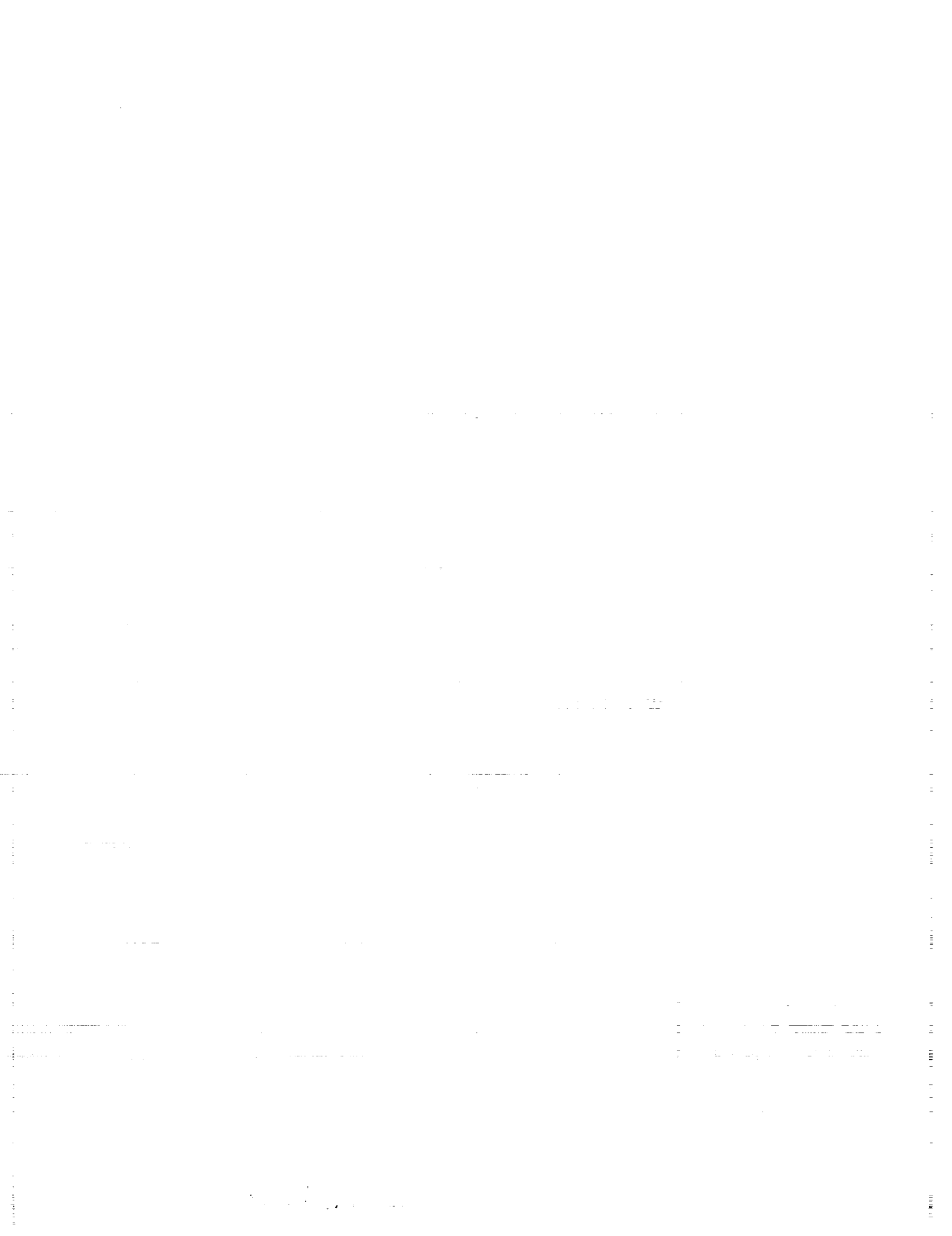


## TABLE OF CONTENTS

	Page
I. INTRODUCTION .....	1
II. DESCRIPTION OF THE EXPERIMENT .....	1
III. DEFINITION AND DESIGN OF THE SERVOS UTILIZED IN SCANNING .....	2
IV. COMPUTER SIMULATION OF THE TOTAL SYSTEM .....	4
V. CONCLUSIONS .....	5
REFERENCES .....	14

## LIST OF ILLUSTRATIONS

Figure	Title	Page
1.	Rotating unbalanced-mass (RUM) mechanical configuration .....	6
2.	Definition of the RUM parameters .....	7
3.	Gimbal angles in relation to the gravity vector .....	7
4.	Servo electronic-hardware block diagram .....	8
5.	Control system block diagram for the RUM servos .....	8
6.	Control system block diagram for the cross-elevation servo .....	9
7.	Control system block diagram for the elevation servo .....	9
8.	Raster scan profile scanning with RUM's and gimbal servos .....	10
9.	RUM rates scanning with RUM's and gimbal servos .....	10
10.	RUM torques scanning with RUM's and gimbal servos .....	11
11.	Gimbal torques scanning with RUM's and gimbal servos .....	11
12.	Gimbal error signals scanning with RUM's and gimbal servos .....	12
13.	Raster scan profile scanning with gimbal servos only .....	12
14.	Gimbal torques scanning with gimbal servos only .....	13
15.	Gimbal error signals scanning with gimbal servos only .....	13

## TECHNICAL PAPER

# DEFINITION AND DESIGN OF AN EXPERIMENT TO TEST RASTER SCANNING WITH ROTATING UNBALANCED-MASS DEVICES ON GIMBALED PAYLOADS

## I. INTRODUCTION

Science instruments aboard balloon-borne platforms, space platforms, and free-flying spacecraft often require that their line-of-sight be repeatedly scanned in some distinct pattern, rather than pointed in a fixed direction. References 1 to 3 give examples of this. In references 4 and 5, a new scheme for scanning such payloads is introduced, one that offers significant power savings in appropriate applications. This scheme relies on the centrifugal force from a pair of rotating unbalanced-mass (RUM) devices to produce the scan motion. To demonstrate the feasibility of this approach, an experiment will be constructed which generates line and raster scans for a gimbaled payload with a pair of RUM devices. This paper describes the experiment and the servos designed to control it. A computer-simulated model of the total system is discussed, and simulation results are presented that predict system performance and verify the control system design.

## II. DESCRIPTION OF THE EXPERIMENT

The RUM experiment consists of an emulated payload mounted in a two-axis, elevation/cross-elevation gimbal system as illustrated in figure 1. Two RUM devices, mounted at opposite ends of the payload, are configured to produce sinusoidal motion about the cross-elevation axis when the RUM's are driven at a constant rate and maintained  $180^\circ$  out of phase. Each RUM has mass,  $m = 0.155$  slugs; on a lever arm,  $r = 0.5$  ft; mounted at a distance,  $d = 2.5$  ft from the center-of-mass of the payload. These parameters, along with the RUM angle  $\theta_R$ , are defined in figure 2. The payload is a steel I-beam with dimensions 6 in by 6 in by 6 ft, weighing about 170 lb. The moments of inertia for the I-beam about the elevation and cross-elevation axes are approximately  $I_E = I_X = 16.3$  slug-ft<sup>2</sup>, respectively. The payload scan frequency in cross-elevation is the same as the frequency of rotation of the RUM devices, in cycles/s or Hz. The scan amplitude is determined from the formula,

$$\theta_{XM} = \frac{2 \cdot m \cdot r \cdot d}{I_X},$$

where  $\theta_{XM}$  is the scan amplitude in rad.<sup>5</sup> Hence, for the parameters given,  $\theta_{XM} = 0.024$  rad. A gimbal servo on the cross-elevation axis centers the scan in this direction. Another servo on the elevation axis maintains a fixed angle during line scans and provides a constant slew rate during raster scans.

Initially, the elevation angle will be commanded to  $\theta_E = 0^\circ$  and the RUM's will generate a line scan. This emulates line scanning in a zero-g environment. Figure 3 describes the elevation and cross-elevation gimbal angles,  $\theta_E$  and  $\theta_X$  respectively, in relation to the gravity vector  $g$ . Once this has been demonstrated, a slow rate in elevation will be superimposed on the line scan to emulate raster scanning in zero-g. The elevation angle will then be commanded to  $\theta_E = -90^\circ$  and the

procedure repeated. Scanning at  $\theta_E = \pm 90^\circ$  is the most difficult situation because the disturbance torques due to gravity on the RUM masses reach their absolute maximum. For a given elevation angle, cross-elevation angle, and RUM angle, the disturbance torque is determined by:

$$T_D = \pm m \cdot g \cdot r \cdot \sin(\theta_E) \cdot \cos(\theta_X + \theta_R),$$

where the + and - signs apply to RUM No. 1 and RUM No. 2, respectively. The acceleration-of-gravity constant has a value of approximately  $g \approx 32.2 \text{ ft/s}^2$ . Hence, at  $\theta_E = \pm 90^\circ$ , the disturbance torque achieves a maximum value of:  $T_{DM} = mgr = 2.5 \text{ ft-lb}$ .

### III. DEFINITION AND DESIGN OF THE SERVOS UTILIZED IN SCANNING

The RUM experiment has four separate, but similar, servos—one for each RUM device and one for each gimbal. All four servos are implemented by a single microcontroller which is the primary component of the electronic-hardware block diagram as shown in figure 4. The microcontroller, an INTEL 80C196KB, performs all the control law computations, while the host computer is used only to program, initialize, and change parameters in the microcontroller during operation. No calculations are performed by the host computer during operation of the RUM experiment.

Each servo has the same basic configuration and components as shown in the shaded portion of figure 4. The microcontroller sends an eight-bit control command to an IXYS IXDP610 pulse-width modulation (PWM) integrated circuit (IC). The IXDP610 outputs a corresponding PWM signal for the power amplifier. The power amplifier receives the PWM signal and generates the current necessary to drive the motor.

The motors are rare-Earth brush type INLAND motor/tachometer units with a motor constant  $K_M = 0.61 \text{ ft-lb}/\sqrt{\text{W}}$  and a ripple torque of about 4 percent. The maximum torque available from each is 11 ft-lb. The tachometers have a sensitivity of 0.48 V/rad/s and a 1-percent ripple voltage.

Motor position is measured using an incremental optical encoder with a home position indicator. The encoders for the experiment are Dynamics Research Corporation model C25 with 3,000 counts/rev. An IXYS IXSE502 encoder interface IC reduces the overhead of the microcontroller by performing a quadrature evaluation of the encoder signals. This increases the overall encoder pulse count to 12,000 counts/rev resulting in a resolution of 0.524 mrad or 1.8 arcmin.

A control system block diagram for the RUM servo is shown in figure 5. A constant incremental angle is commanded every  $T = 5 \text{ ms}$ , resulting in a constant rate of rotation. For compatibility, the commanded value entered into the microcontroller is chosen to be an integer multiple of the incremental encoder quantization. To properly generate line scans, the two RUM devices need to be  $180^\circ$  out of phase with each other. This is accomplished by initially positioning the RUM's and then commanding the same incremental angles to each device. Feed-forward compensation is used to cancel the disturbance torque due to gravity acting on the RUM mass before it produces a rate and angle error.

Control system block diagrams for the cross-elevation and elevation servos are shown in figures 6 and 7, respectively. The function of the cross-elevation servo is to keep the scan centered



on the target, and the elevation servo is used for raster scanning. Rate feedback is required from the tachometers for control of both gimbals axes. The tachometer outputs are filtered by 40-Hz analog low-pass filters before being sampled by 10-bit A/D converters in the microcontroller. The A/D converters are scaled to a range of  $\pm 0.35$  rad/s. To measure the gimbal angles, the gimbal encoder outputs are also sampled every 5 ms and summed in the microcontroller. In order to synchronize the cross-elevation servo with the RUM servos, the commands to the cross-elevation servo are generated from the RUM servo commands and the ideal scan parameters. The elevation servo differs from the cross-elevation servo only in the input commands. In elevation, zero rate is commanded for line scanning and a nonzero constant rate is commanded for raster scanning.

The control gains for the RUM servos were chosen for a 5-Hz unity gain crossover frequency, and those for the gimbal servos were chosen for 0.25 Hz. These were arrived at by simulation, subject to the condition that they be separated by a factor of 10 or more to prevent the possibility of any cross coupling between the servos. In order to achieve excellent results, the sampling rate for the sensors was chosen to be 200 Hz (i.e., 5 ms) which is more than a factor of 10 above the unity gain crossover frequency for the RUM servos. For these design specifications, the RUM servo control gains were determined to be:

$$k_R = 6,500.0 \text{ s}^{-2}$$

$$k_P = 260.0 \text{ s}^{-2}$$

$$k_I = 2.6 \text{ s}^{-2}$$

$$\hat{I}_R = 0.03875 \text{ slug-ft}^2,$$

and the control gains for the gimbal servos were determined to be:

$$k_R = 15.7 \text{ s}^{-1}$$

$$k_P = 1.59 \text{ s}^{-1}$$

$$k_I = 0.00125 \text{ s}^{-1}$$

$$\hat{I}_X = \hat{I}_E = 16.3 \text{ slug-ft}^2.$$

Finally, the torque motor commands for the gimbal servos are passed through a 40-Hz digital low-pass filter before the PWM commands are generated. This helps attenuate any higher frequency noise in the gimbal servos. The digital filter parameters were calculated to be :

$$a = 0.285$$

$$b = 0.715.$$

#### IV. COMPUTER SIMULATION OF THE TOTAL SYSTEM

A computer model of the system was developed to verify the servo designs and make an assessment of system performance. The plant is modeled using simple rigid-body dynamics. The torque motor models include torque ripple and brush friction. The latter is simulated by a Dahl friction model with a running friction of  $T_F = 0.25$  ft-lb. The quantization associated with the system's sensors and motors is also included, as well as the sample rate of the sensors and computation cycle of the microcontroller.

Figure 8 shows a raster scan generated by simulation. The elevation angle starts at  $\theta_E = -\pi/2$  rad or  $-90^\circ$ , and the cross elevation axis is given a sinusoidal command with a frequency of 1 Hz and an amplitude of  $\theta_{XM} = 0.024$  rad or  $1.4^\circ$ . The elevation axis is rotated at a constant rate equal to  $\Omega_E = 0.011$  rad/s or  $0.6^\circ/\text{s}$ . The rotation rates of the RUM devices are shown in figure 9. The RUM's are initially at rest and then commanded to a rate of  $\Omega_R = 6.28$  rad/s, or 1 Hz, to generate the scan. The torque motor outputs for the RUM devices are shown in figure 10. The peak torque value is 2.75 ft-lb. Figure 11 shows the cross-elevation gimbal torque, which keeps the scan centered and counters gimbal friction. At steady state, its peak value is 0.5 ft-lb. Figure 11 also shows the torque required by the elevation servo to overcome friction and provide a constant slew rate. After the initial transient, its peak value is 0.35 ft-lb. Figure 12 shows the gimbal angle error signals. At steady state, the peak cross-elevation error is 0.001 rad or  $0.06^\circ$ , while the peak elevation error is 0.0008 rad or  $0.05^\circ$ .

These simulation results can be used to estimate the power savings realized by using the RUM devices for scanning, as opposed to scanning solely with the gimbal torquers. With a motor constant of  $0.61 \text{ ft-lb}/\sqrt{\text{W}}$ , the peak power for scanning with the RUM devices is calculated to be:

$$P_M = 2 \cdot (2.75/0.61)^2 + (0.5/0.61)^2 + (0.35/0.61)^2 = 42 \text{ W}.$$

For comparison, this same case was simulated using only the gimbal servos to perform the scan motions without the activating the RUMs. To accomplish this, it was first necessary to increase the maximum torque from the gimbal torquers from 11 ft-lb to 22 ft-lb to prevent the cross-elevation torquer from saturating while scanning. The simulation results are shown in figures 13 through 15. Figure 13 shows the raster scan profile and figure 14 presents the gimbal torques. Observe that the peak cross-elevation torque is now 16.0 ft-lb, as opposed to 0.5 ft-lb before. The peak elevation torque remains unchanged at 0.35 ft-lb. The gimbal angle error signals are presented in figure 15. Observe that the peak cross-elevation error signal is now 0.009 rad or  $0.52^\circ$ , compared to 0.001 rad or  $0.06^\circ$  before. The peak elevation error signal remains unchanged at 0.0008 rad or  $0.05^\circ$ . Therefore, scanning without the RUM's increases the peak cross-elevation torque by a factor of 32 and the peak cross-elevation error signal by a factor of 9. The peak power for this case yields:

$$P_M = (16.0/0.61)^2 + (0.35/0.61)^2 = 688 \text{ W}.$$

Thus, when comparing the peak powers for scanning in a one-g environment, the RUM devices are 16 times more efficient. Furthermore, because the gravity torque is zero in a one-g environment at  $0^\circ$  elevation angle or in a zero-g environment, using the RUM devices for scanning reduces the power required by a factor of 688. Table 1 presents the power requirements for each scenario.

Table 1. Peak power required for scanning.

Conditions	RUMs+Gimbals (W)	Gimbals Only (W)
1-g Environment/ $\pm 90^\circ$ Elevation Angle	42	688
1-g Environment/ $0^\circ$ Elevation Angle	1	688
0-g Environment/All Elevation Angles	1	688

## V. CONCLUSIONS

The results from the computer simulation indicate that the servo designs chosen for the RUM experiment work well for generating both line and raster scans. The mechanical configuration can simulate scanning in both zero-g and one-g environments. Even in the worst-case orientation of one-g, the power required is 16 times less when using the RUM devices to produce the scan motion.

The plan for the future is to implement the experimental design presented here in actual mechanical and electrical hardware and software. Tests will be performed on the physical system as soon as the actual components have been designed, fabricated, and integrated. The actual power required for scanning with and without the RUM devices will be determined, and these results will be analyzed and compared with the simulation results presented in this paper.

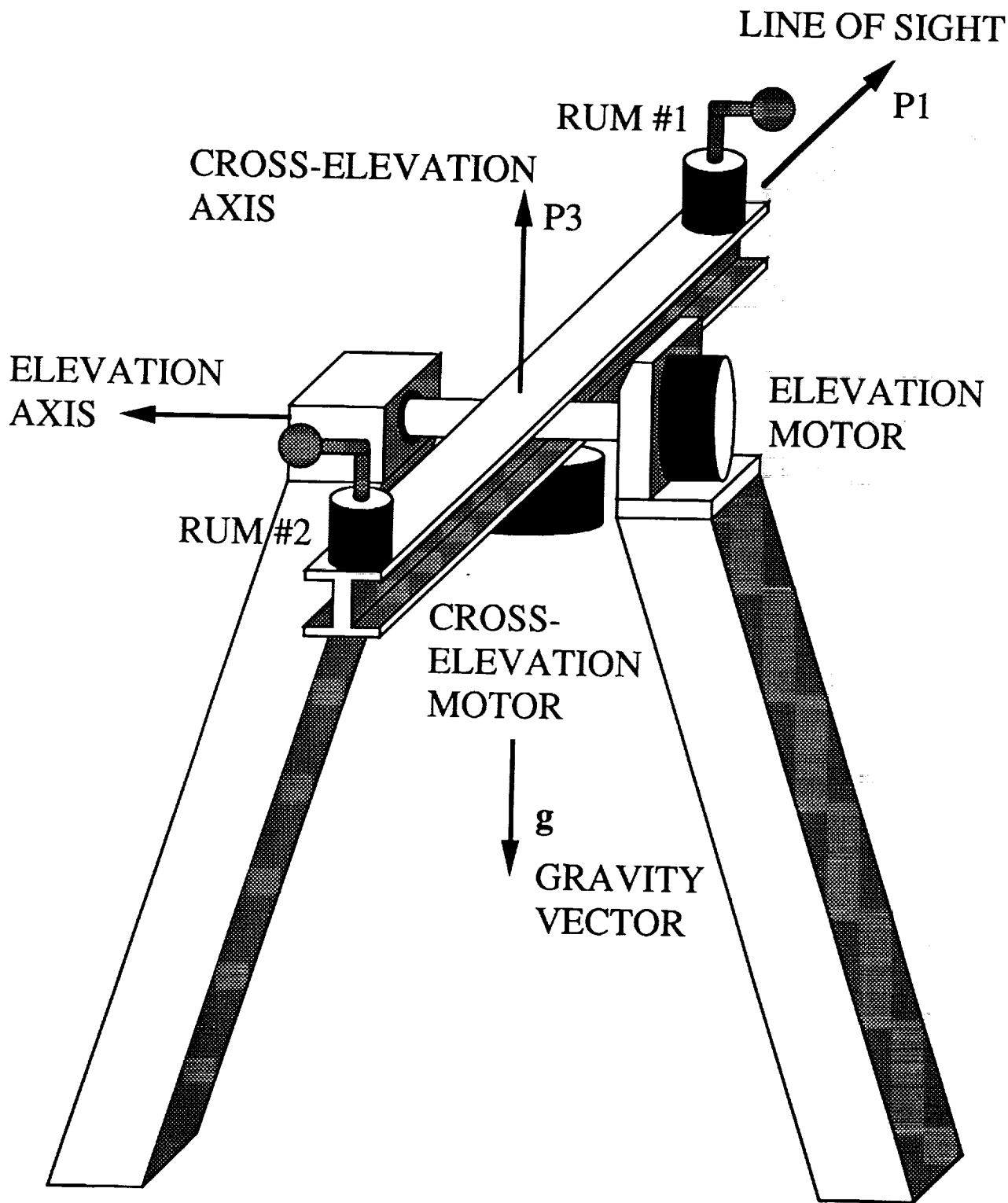


Figure 1. Rotating unbalanced-mass (RUM) mechanical configuration.

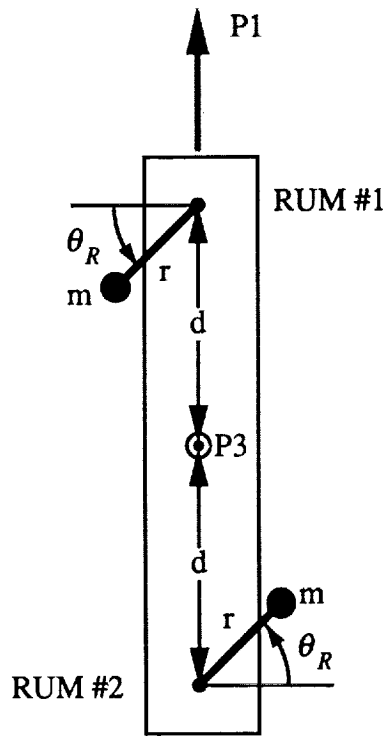


Figure 2. Definition of the RUM parameters.

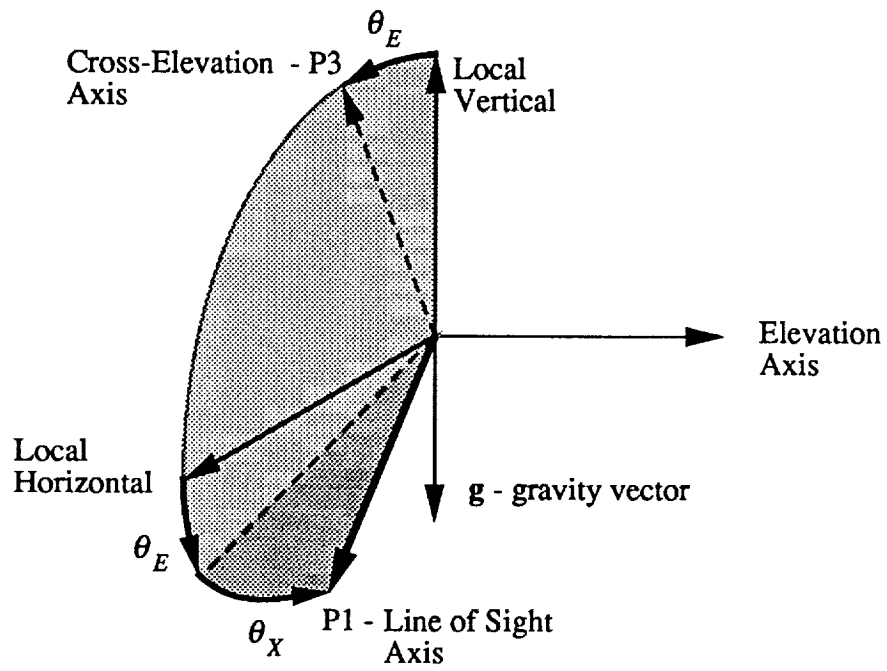


Figure 3. Gimbal angles in relation to the gravity vector.

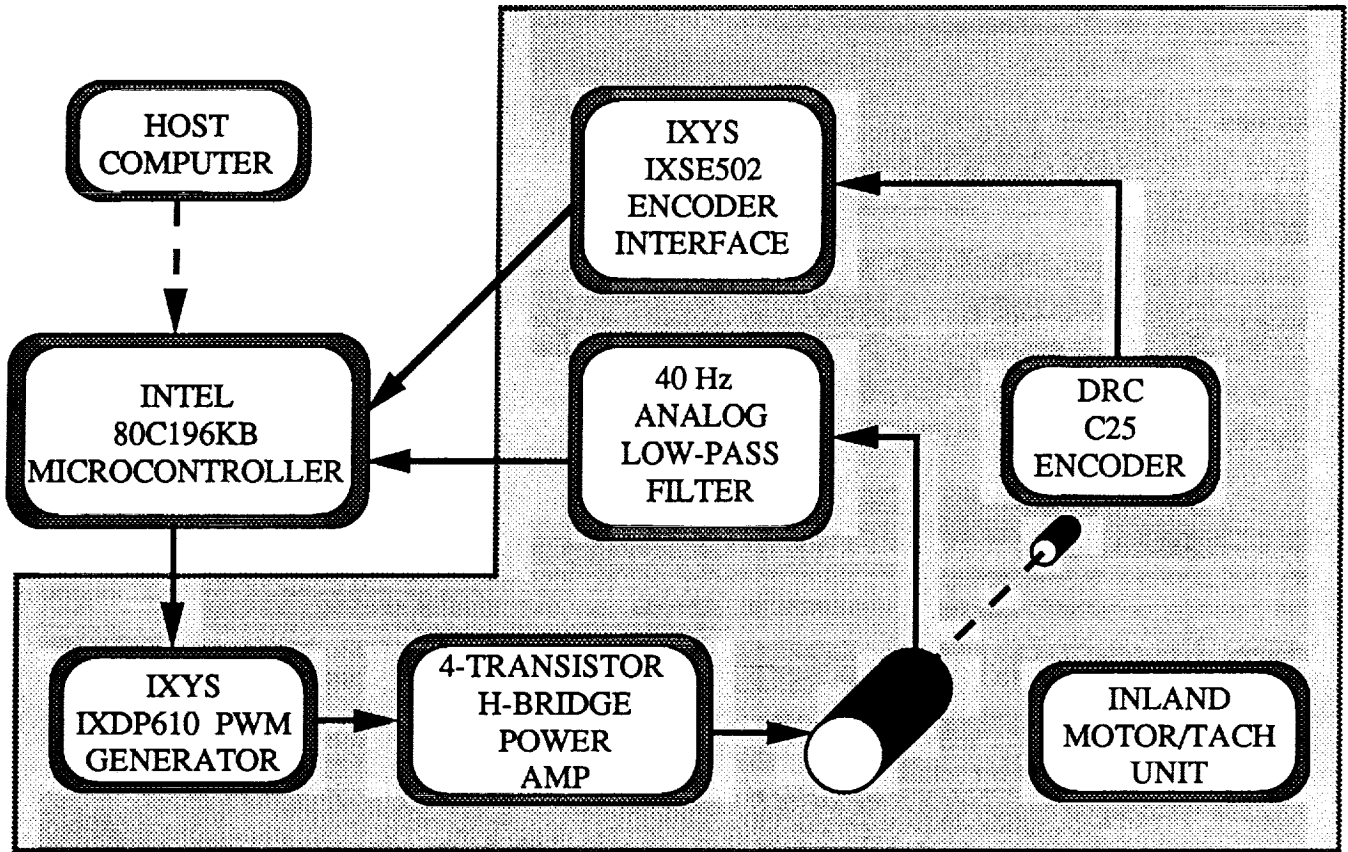


Figure 4. Servo electronic-hardware block diagram.

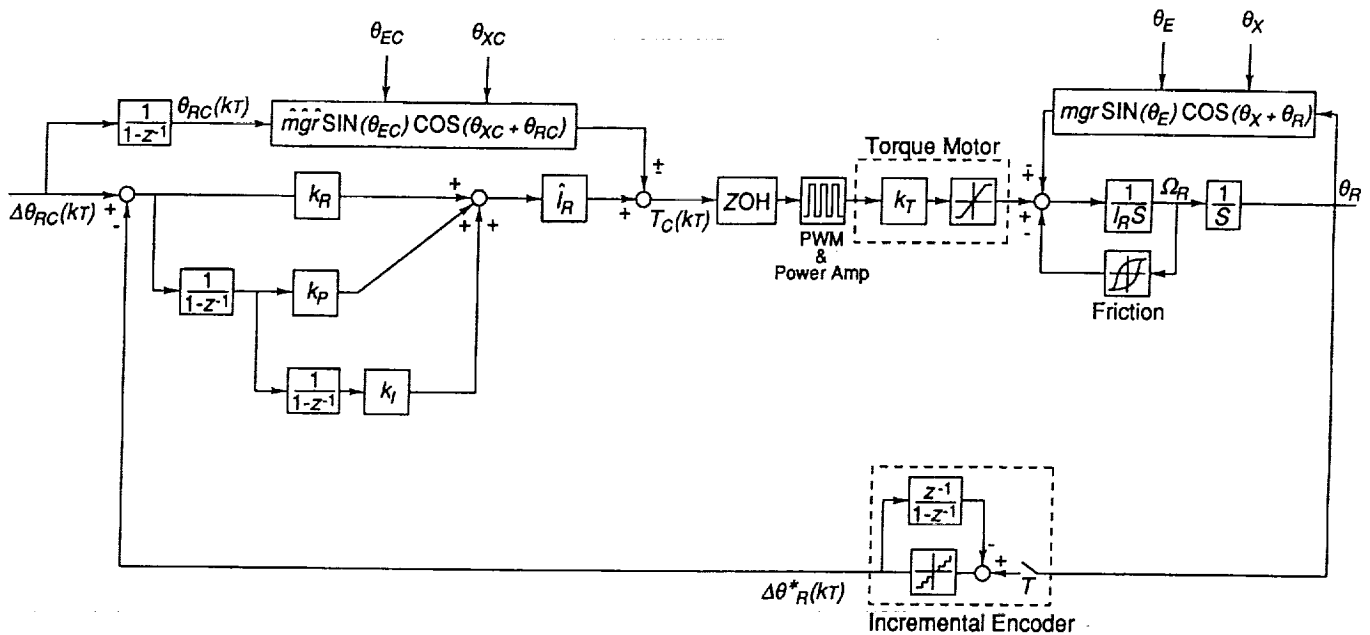


Figure 5. Control system block diagram for the RUM servos.

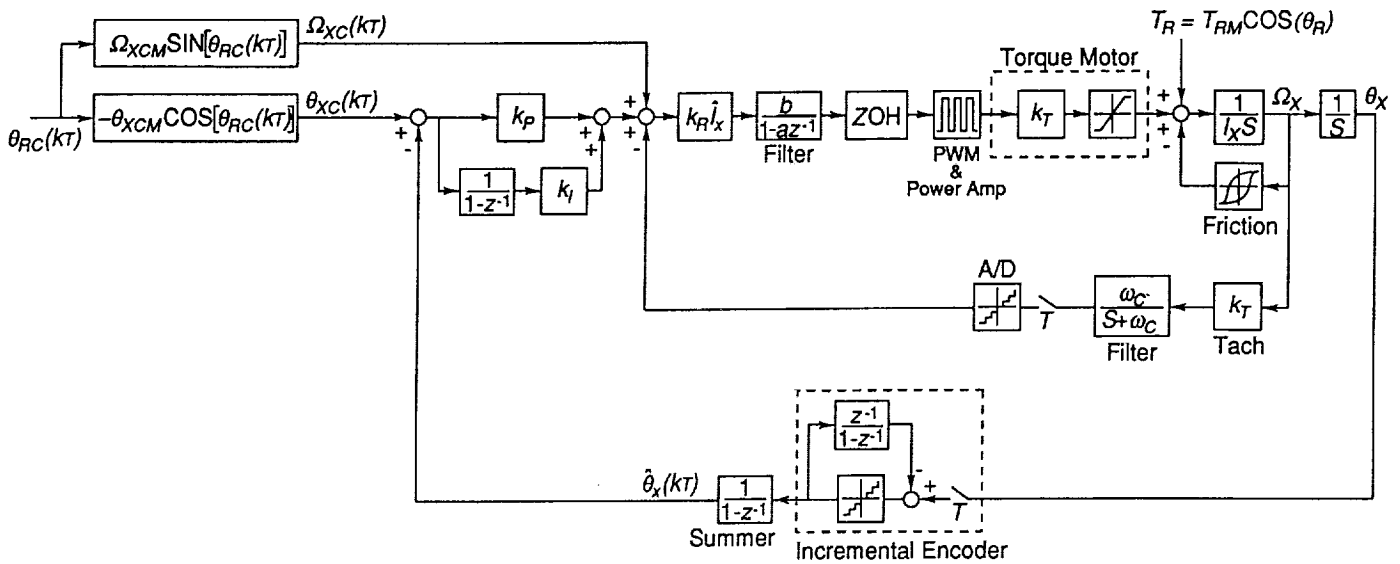


Figure 6. Control system block diagram for the cross-elevation servo.

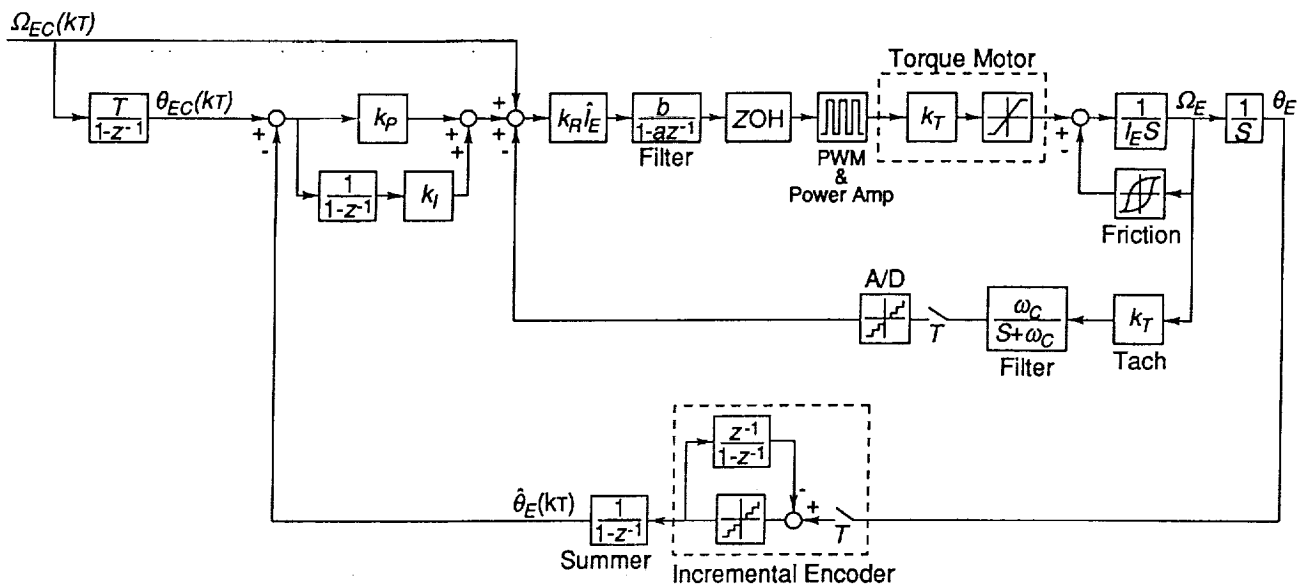


Figure 7. Control system block diagram for the elevation servo.

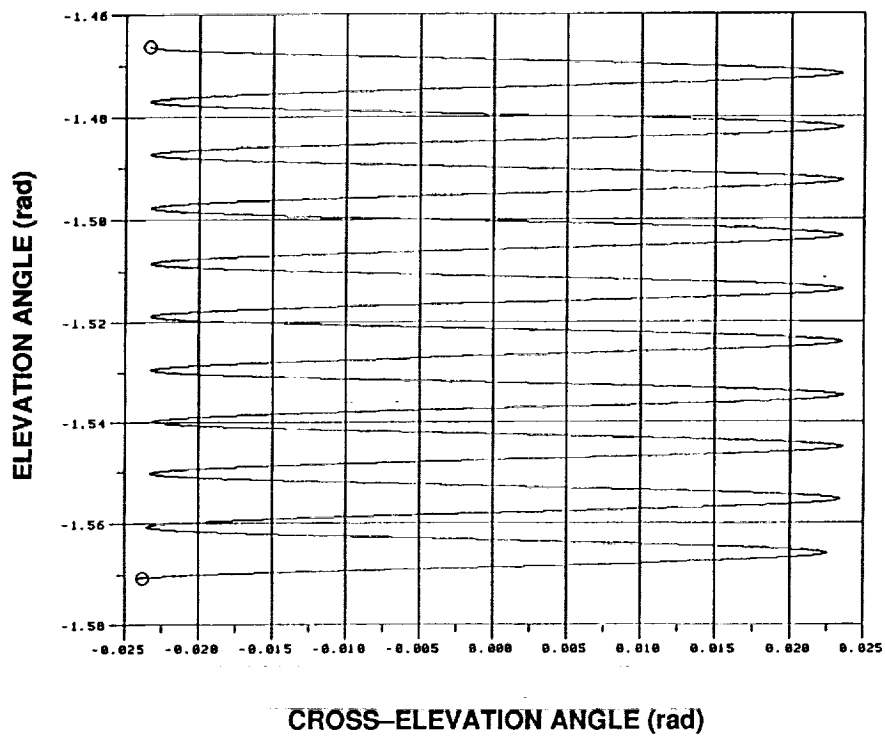


Figure 8. Raster scan profile scanning with RUM's and gimbal servos.

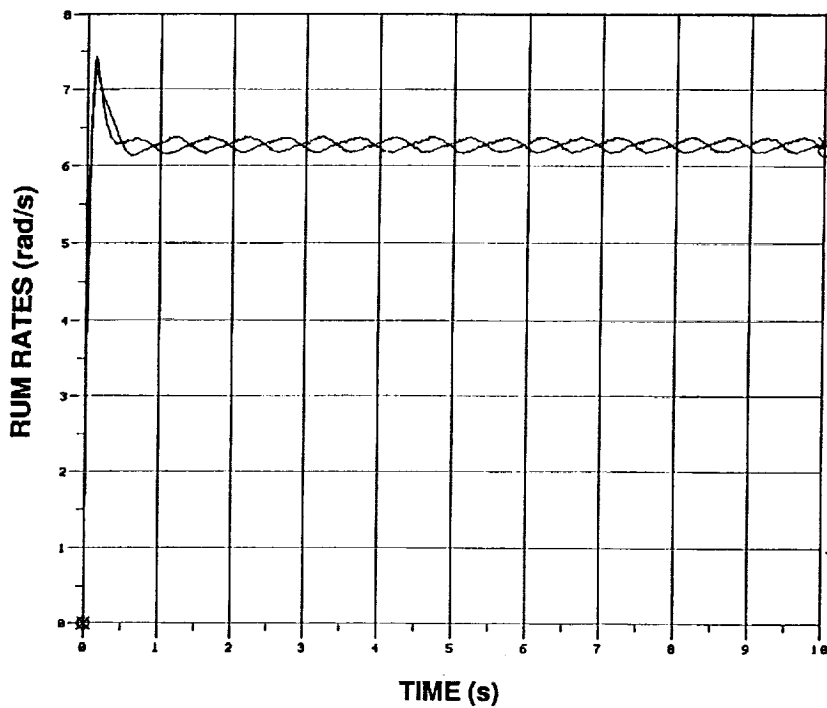


Figure 9. RUM rates scanning with RUM's and gimbal servos.



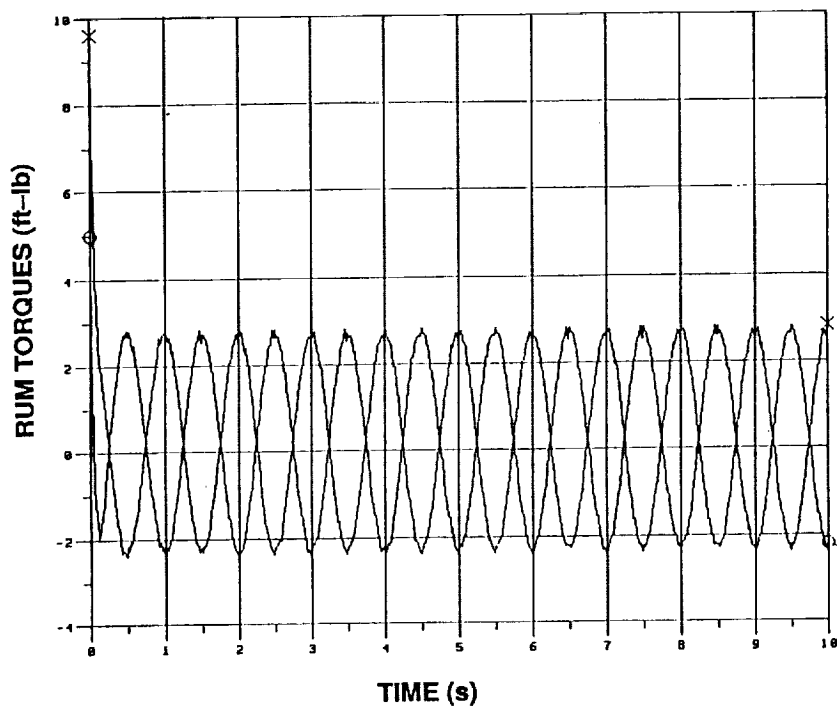


Figure 10. RUM torques scanning with RUM's and gimbal servos.

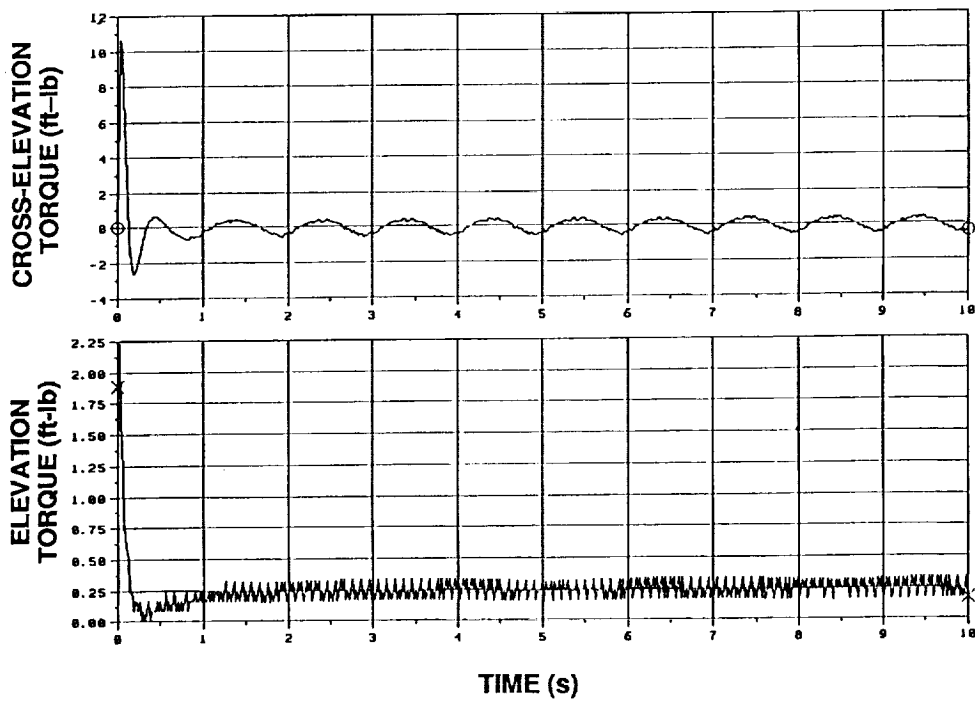


Figure 11. Gimbal torques scanning with RUM's and gimbal servos.

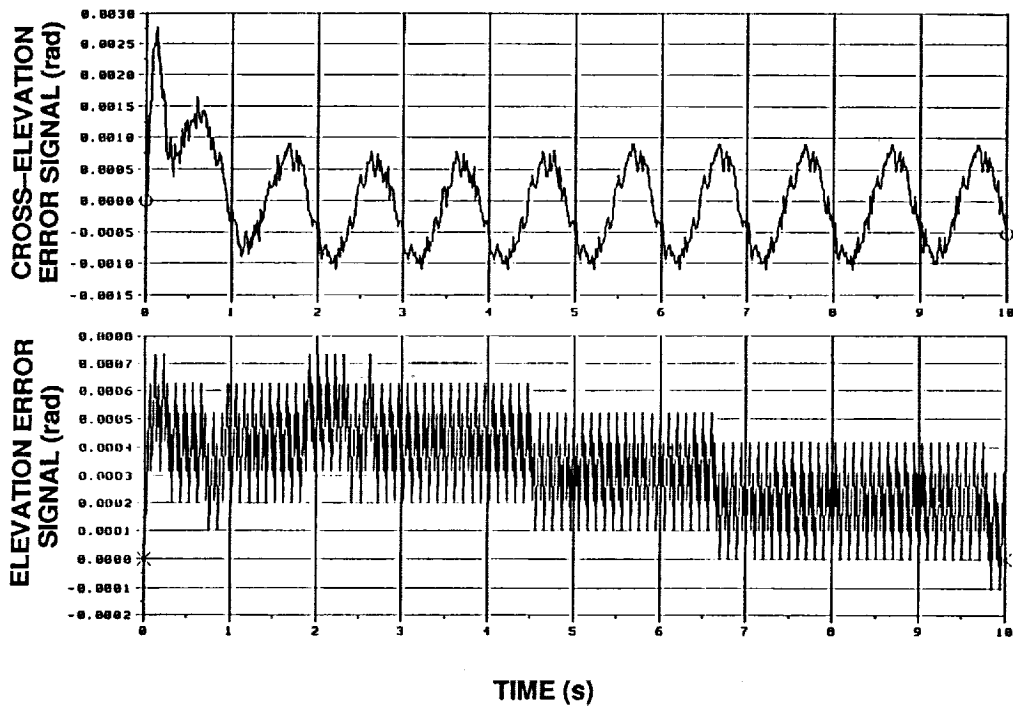


Figure 12. Gimbal error signals scanning with RUM's and gimbal servos.

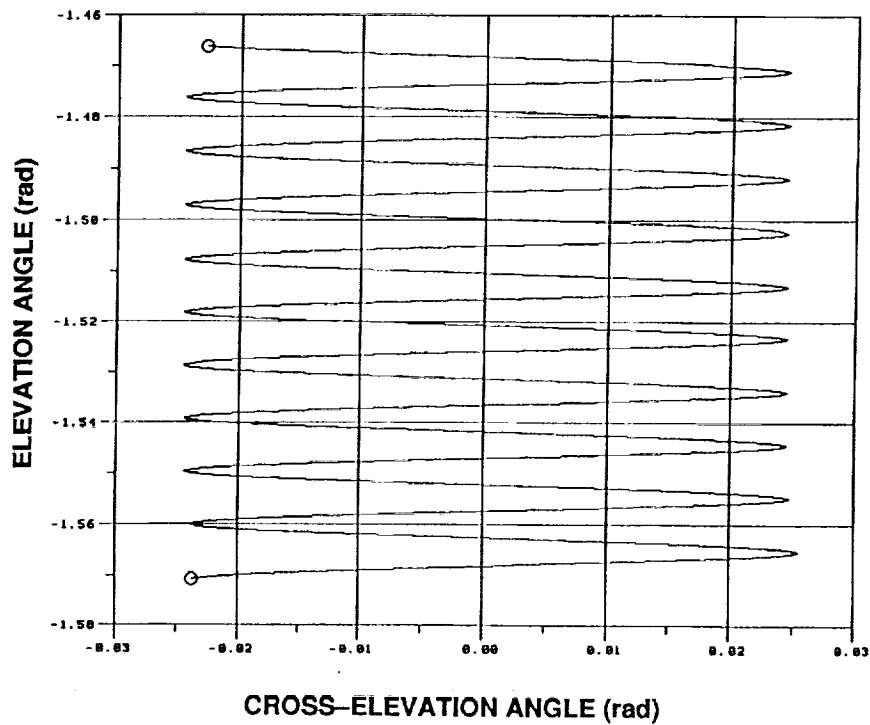


Figure 13. Raster scan profile scanning with gimbal servos only.

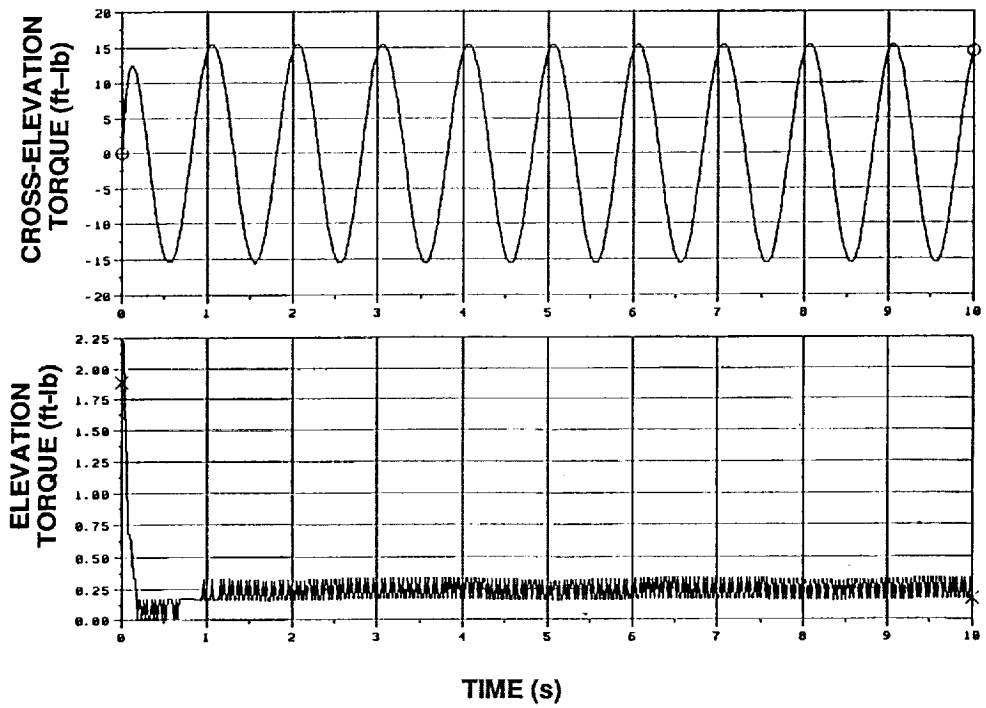


Figure 14. Gimbal torques scanning with gimbal servos only.

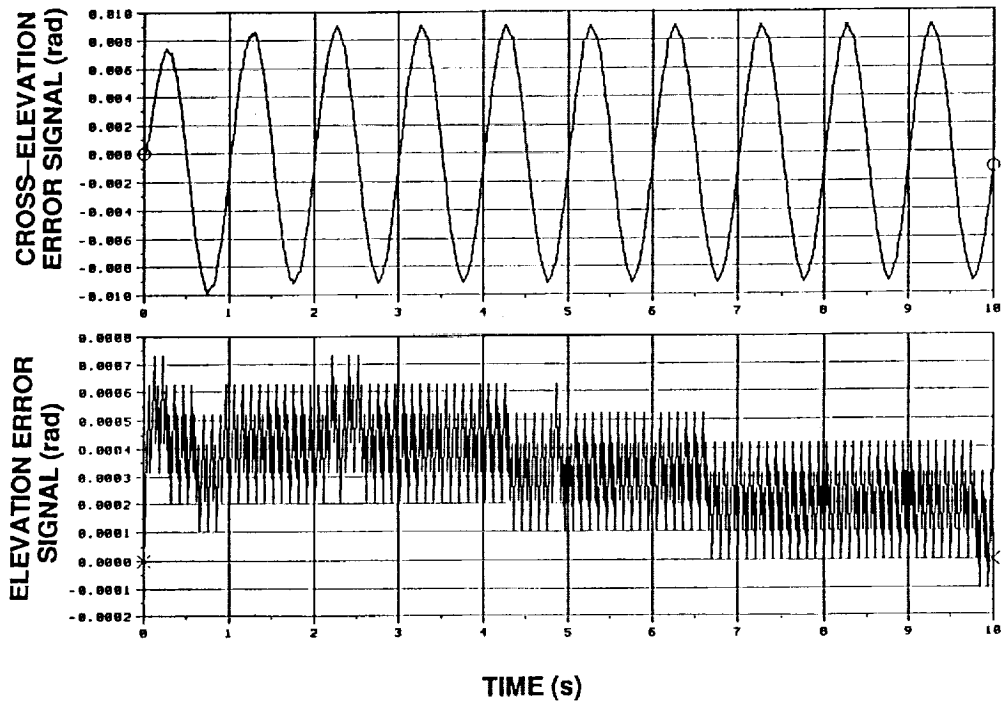


Figure 15. Gimbal error signals scanning with gimbal servos only.

## REFERENCES

1. "The GRID on a Balloon Definition Study Report." NASA Goddard Space Flight Center, Greenbelt, MD, June 14, 1989.
2. "Space Telescope Moving Target and Scan Pointing Capability Error Budget, ST/SE-24, Section H, Part 4." LMSC/FO61415, Lockheed Missiles and Space Company, Sunnyvale, CA, October 21, 1985.
3. Nein, M.E., and Nicaise, P.D.: "Experiment Pointing Subsystems (EPS) Requirements for the Spacelab Missions." NASA TM X-64978, NASA Marshall Space Flight Center, AL, December 1975.
4. Polites, M.E.: "Rotating-Unbalanced-Mass Devices for Scanning Balloon-Borne Experiments, Free-Flying Spacecraft, and Space Shuttle/Space Station Experiments." NASA TP-3030, NASA Marshall Space Flight Center, AL, June 1990.
5. Polites, M.E.: "New Method for Scanning Spacecraft and Balloon-Borne/Space-Based Experiments." Journal of Guidance, Control and Dynamics, vol. 14, No.3, May-June 1991, pp. 548-553.



REPORT DOCUMENTATION PAGE			Form Approved OMB No. 0704-0188	
Public reporting burden for this collection of information is estimated to average 1 hour per response, including the time for reviewing instructions, searching existing data sources, gathering and maintaining the data needed, and completing and reviewing the collection of information. Send comments regarding this burden estimate or any other aspect of this collection of information, including suggestions for reducing this burden, to Washington Headquarters Services, Directorate for Information Operations and Reports, 1215 Jefferson Davis Highway, Suite 1204, Arlington, VA 22202-4302, and to the Office of Management and Budget, Paperwork Reduction Project (0704-0188), Washington, DC 20503.				
1. AGENCY USE ONLY (Leave blank)	2. REPORT DATE June 1992	3. REPORT TYPE AND DATES COVERED Technical Paper		
4. TITLE AND SUBTITLE Definition and Design of an Experiment To Test Raster Scanning With Rotating Unbalanced-Mass Devices on Gimbaleed Payloads			5. FUNDING NUMBERS	
6. AUTHOR(S) W.D. Lightsey, D.C. Alhorn, and M.E. Polites				
7. PERFORMING ORGANIZATION NAME(S) AND ADDRESS(ES) George C. Marshall Space Flight Center Marshall Space Flight Center, Alabama 35812			8. PERFORMING ORGANIZATION REPORT NUMBER  M-691	
9. SPONSORING / MONITORING AGENCY NAME(S) AND ADDRESS(ES) National Aeronautics and Space Administration Washington, DC 20546			10. SPONSORING / MONITORING AGENCY REPORT NUMBER  NASA TP-3249	
11. SUPPLEMENTARY NOTES Prepared by the Structures and Dynamics Laboratory and the Information and Electronic Systems Laboratory, Science and Engineering Directorate.				
12a. DISTRIBUTION / AVAILABILITY STATEMENT Subject Category: 31 Unclassified — Unlimited			12b. DISTRIBUTION CODE	
13. ABSTRACT (Maximum 200 words)  This paper describes an experiment designed to test the feasibility of using rotating unbalanced-mass (RUM) devices for line and raster scanning gimbaleed payloads, while expending very little power. The experiment is configured for ground-based testing, but the scan concept is applicable to ground-based, balloon-borne, and space-based payloads, as well as free-flying spacecraft. In this paper, the servos used in scanning are defined, the electronic hardware is specified, and a computer simulation model of the system is described. Simulation results are presented that predict system performance and verify the servo designs.				
14. SUBJECT TERMS Free-Flying Spacecraft, Gimbaleed Payloads, Line Scanning, Raster Scanning, Rotating Unbalanced-Mass Devices			15. NUMBER OF PAGES 18	
			16. PRICE CODE A03	
17. SECURITY CLASSIFICATION OF REPORT Unclassified	18. SECURITY CLASSIFICATION OF THIS PAGE Unclassified	19. SECURITY CLASSIFICATION OF ABSTRACT Unclassified	20. LIMITATION OF ABSTRACT Unlimited	